To direct the self-assembly of AIEgens by three-gear switch: Morphology study, amine sensing and assessment of meat spoilage

Jingqi Han[a], Yaping Li[a], Jing Yuan[a], Zhongfeng Li[a], Ruixue Zhao[a], Tianyu Han[a,*], Tiandong Han[b,**]

[a] Department of Chemistry, Capital Normal University, 100048, Beijing, PR China
[b] Beijing Friendship Hospital, Capital Medical University, 100048, Beijing, PR China

ARTICLE INFO

ABSTRACT

In this study, we synthesized a class of positional isomers by attaching a carboxylic group in different sites (para-, meta- and ortho-position) of an aromatic core. The isomers undergo both aggregation-induced emission (AIE) and intramolecular charge transfer (ICT) mechanisms, as proved by their photoluminescence (PL) behaviour. Changing the position of the carboxylic group will adjust the dipole–dipole direction, which further controls the self-assembled architecture: The morphology undergoes a transition from 1D nanowire to 2D microsheet, and even to 3D microcube. The benzoic acid moiety of the AIE isomers has strong affinity to amines, and adsorbing amines leads to spectral changes including hypochromatic shift and emission quenching. The sensing mechanism was studied by density functional theory (DFT), which reveals that the amine-responsive fluorescence can be ascribed to the weakened ICT effect. A prototype of amine sensor based on m-DB self-assemblies was developed accordingly, showing a remarkable quenching efficiency as high as 85.4%. A linear relation was obtained from the quantitative determination of amine, offering a low detection limit of 2.02 Pa. It can also respond to other organic amines such as diisopropylamine (DIPA), triethylamine (TEA), isopropylamine (IPA) and cyclohexylamine (CHA). Finally, the practicality of the sensor was also demonstrated: When placing the sensing film beside the spoiled meat, the spectrum shows a remarkable fluorescence quenching; in contrast, fresh meat samples have induced a much lower quenching efficiency. This demonstrates that the AIE isomers have a great potential to serve as indicators for meat spoilage.

© 2017 Elsevier B.V. All rights reserved.

1. Introduction

In view of recent development of nano/microtechnologies, the design and creation of nano/micro-sized materials made of self-assembled molecules is becoming of acute interest, as it offers a bottom-up approach to build well-defined architectures to endow the nano/micromaterials with a variety of functions [1–3]. Intensive investigations have shown that advances in optical sensors benefit tremendously from the high-ordered structure and easy fabrication of molecular assemblies [4–6]. In search of the building blocks for optical functional materials, aggregation-induced emission (AIE) systems are emerged as a quickly growing field, as they have avoided intermolecular π-π stacking by twisting the molecular conformation, thus the solid emission could be remarkably enhanced [7]. The rapid expansion of AIE luminogens (AIEgens) with a clear mechanism model has motivated researchers to further developed AIE building blocks for supramolecular assemblies with diverse morphologies, including nanorods [8], nanofibers [9], nanoladders [10], nanospheres [11,12], and helical structures [13], *etc.* Studying the effect of substituents is of great significance for providing information on the relationships between supramolecular structures and properties, from which we can get insights into the working mechanisms and further modify or improve the performances of the isolated molecules, including AIEgens [14–16].

To create an AIEgen for self-assembly, the substituent group offering weak forces should be seriously considered. The commonly used condensed ring might be a double-edged sword in the case of assembly: They arrange themselves in high order to form a disk-like architecture via π-π interactions on one hand, but promote the formation of excimers and exciplexes on the other hand, resulting in the undesired quenching effect [17,18]. B.Z. Tang and Z. Zhao, et al. have reported that the incorporation of polycyclic aromatic hydrocarbons into AIE cores will lower the emission efficiency in the aggregated state [19]. An alternative approach is incorporat-

---

* Corresponding author.
** Corresponding author at: Beijing Friendship Hospital, Capital Medical University, 100048, Beijing, PR China.
 E-mail addresses: phanw@163.com (T. Han), cruiser412@163.com (T. Han).
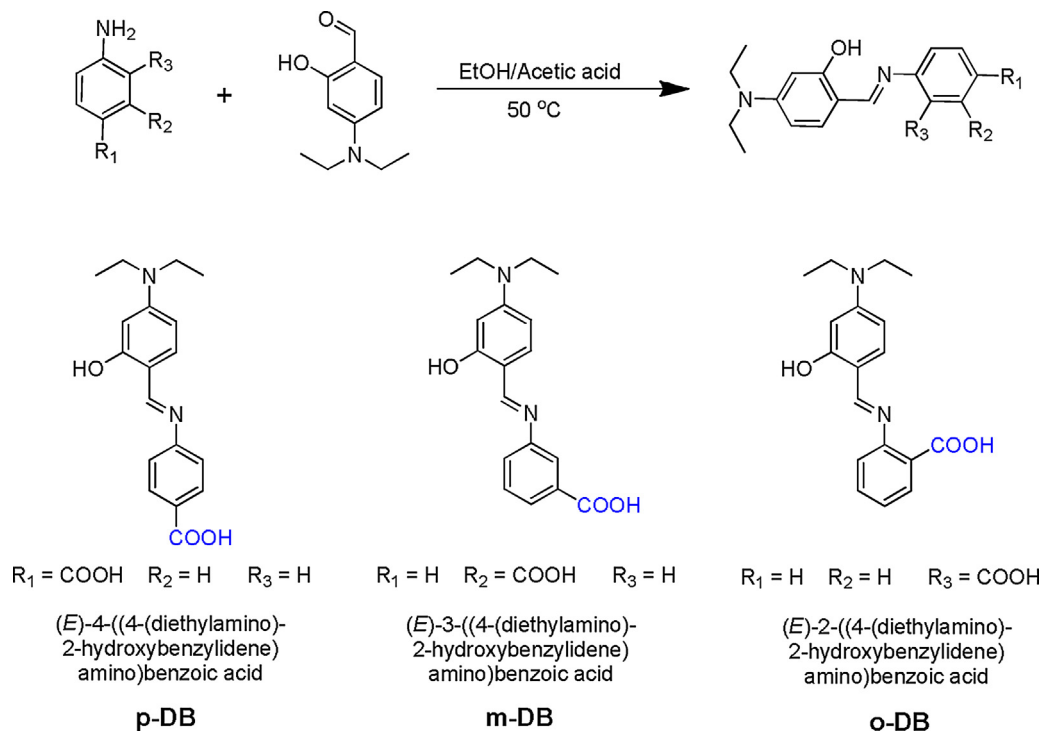
Scheme 1. Synthetic route and chemical structures of p-, m- and o-DB.

ing electron donor (D) and acceptor (A) units to AIE cores to create highly polarized compounds with large dipole–dipole interactions [20,21]. This approach may activate both AIE and intramolecular charge transfer (ICT) properties [22–24]. Besides, it dispenses with the dilemma of conjugation-rotation, and further lowers the energy gap between ground and excited state, favoring both high solid quantum efficiency and remarkable bathochromic-shift in absorption/emission wavelength [25]. Another advantage intrinsic to D-A units stems from their diversity and compatibility, in other words, there is a wide variety of D-A units for our choice when fabricating D-A type AIEgens, and to which position do they link seems to be a free-choice if steric effect permits.

In this work, we attached the carboxylic group in different positions , meta- and ortho-position) of an AIE core to yield positional isomers with self-assembly behaviour. We systematically investigated the self-assembled patterns of the isomers. The dipole–dipole interactions are severely impacted by the relative location of D-A units, leading the molecules to assemble in entirely different ways. The morphology of the AIEgens transforms from one-dimensional (1D) to two-dimensional (2D), and further to three-dimensional (3D) nano/micro structures, exhibiting strong position-dependence. The assemblies show remarkable fluorescence responses toward amines, offering great potential to be fabricated into portable sensors for detecting meat spoilage.

2. Experimental section

2.1. Instruments and methods

Chemicals were purchased from J&K Scientific and used as received without further purification. ^{1}H and ^{13}C NMR spectra were measured on a Varian VNMRS 600 MHz spectrometer using tetramethylsilane as the internal reference. Photoluminescence (PL) spectra were recorded on a HITACHI F-7000 FL spectrophotometer. High resolution mass spectra (HRMS) were recorded on a GCT premier CAB048 mass spectrometer operated in MALDI-TOF mode. The fluorescence quantum yields (Φ_F) were determined

using an Edinburgh FLS920 steady/transient state fluorescence spectroscope equipped with calibrated integrating sphere. UV–vis spectra were recorded on a SHIMADZU UV 2550 spectrophotometer. The morphologies of the material were investigated by using a Hitachi SU-8010 scanning electron microscope (SEM). Fluorescence images were captured under an Olympus CKX41 phase contrast microscope with 365 nm irradiation. The ground-state geometries were optimized using DFT with B3LYP/cc-pVDZ basis set. All the calculations were performed using Gaussian 05 package.

2.2. Synthesis and structural characterization

Synthesis and structural characterization of (*E*)-4-((4-(diethylamino)-2-hydroxybenzylidene)amino)benzoic acid (*p*-DB) and (*E*)-2-((4-(diethylamino)-2-hydroxybenzylidene) amino)benzoic acid (o-DB) can be found in our previous publications [24]. Detailed synthetic process of (*E*)-3-((4-(diethylamino) −2-hydroxybenzylidene)amino)benzoic acid (m-DB) is given as follows (Scheme 1). To a round-bottom flask (150 mL) were added 4-(diethylamino)-2-hydroxybenzaldehyde (1.00 g, 5.17 mmol), 4-aminobenzoic acid (0.71 g, 5.17 mmol) and 100 mL dehydrated ethanol. Two drops of acetic acid were added to the reaction mixture before it was heated to 50 °C. After stirring for 10 h, the reaction was cooled to room temperature. Then the formed precipitates were collected by vacuum filtration using dehydrated ethanol to rinse. No further purification was needed. Yield: 52.5%. ^{1}H and ^{13}C NMR spectrum of m-DB are shown in Fig. S1 and S2 , respectively. ^{1}H NMR (400 MHz, DMSO-d_6), δ (ppm): 13.39 (br s, 1H), 12.95 (br s, 1H), 8.73 (s, 1H), 7.78 (s, 1H), 7.75–7.74 (d, 1H), 7.54–7.51 (d, 1H), 7.49–7.48 (t, 1H), 7.36–7.34 (d, 1H), 6.32–6.30 (dd, 1H), 6.06 (d, 1H), 3.39–3.36 (q, 4H), 1.11–1.09 (t, 6H). (Abbreviations: br = broad, s = singlet, d = doublet, t = triplet, q = quartet). ^{13}C NMR (151 MHz, DMSO-d_6), δ (ppm): 167.54, 163.71, 162.71, 152.16, 149.15, 134.88, 132.51, 130.05, 126.58, 125.74, 121.69, 108.98, 104.38, 97.21, 44.37, 12.96. HRMS (MALDI-TOF): *m/z* 313.1546 [(M + H)$^+$, calcd 313.1552].